

Solution Characterization, Conformation Analysis, and Dynamics of the Ligand 1,1'-Bis(diphenylphosphino)ferrocene (dppf) in $\text{Re}_2(\mu\text{-OMe})_2(\mu\text{-dppf})(\text{CO})_6$

Sik-Lok Lam, Yu-Xin Cui,[†] and Steve C. F. Au-Yeung*

Department of Chemistry, The Chinese University of Hong Kong, Shatin, New Territories, Hong Kong

Yaw-Kai Yan and T. S. Andy Hor*

Department of Chemistry, Faculty of Science, National University of Singapore, Kent Ridge 0511, Singapore

Received November 30, 1993*

The dynamic process involving the diphenyls (ϕ , ϕ') in 1,1'-bis(diphenylphosphino)ferrocene (dppf) in $[\text{Re}_2(\mu\text{-OMe})_2(\mu\text{-dppf})(\text{CO})_6]$ at 228 K is characterized by conformational analysis. At this temperature, the fluxionality of the dppf ligand ceases whereas the dynamics of the phenyl rings about the P-C_{ipso}(ϕ, ϕ') (the "ipso" in the phenyl rings) was rapid on the NMR time scale down to -85 °C. The fluxional barrier ($\Delta G^*_{\text{exp}} = 46.4 \pm 1.0$ kJ/mol) for the interconversion of the *R* and the *S* forms was determined by variable-temperature ¹H NMR spectroscopic studies. The range of the Cp proton chemical shifts varies from $\delta(^1\text{H}) = 3.00$ to 5.68 ppm and is the largest reported. The $[\text{Re}_2(\mu\text{-OMe})_2]$ core was found to be static throughout the temperature-lowering process indicating that fluxionality is thus confined to the dppf fragment in the molecule. Ring current effects similar to those observed for the internal protons (H_i) in cyclophane molecules are attributed to be responsible for the anomalous proton shifts. Molecular modeling calculations indicate complete ring flipping of the diphenyls about their respective P-C_{ipso} bonds was not possible because of the steric congestion about the ferrocene. The torsional twist of the diphenyls about their P-C_{ipso} bonds was correlated, restricted, and in opposite directions. The ranges for the torsional angles ϕ'_t and ϕ_t were determined respectively to be $92.6^\circ \leq \phi'_t \leq 112.4^\circ$ and $147.6^\circ \leq \phi_t \leq 177.8^\circ$.

Introduction

Ferrocene-based diphosphine complexes such as 1,1'-bis(diphenylphosphino)ferrocene (dppf) have been shown to be useful ligands because of their tunable stereogeometries, variable coordination modes,^{1–8} and the electrochemical⁹ and catalytic^{10–20} activities brought to their complexes. The skeletal flexibility of dppf is of particular importance as it represents the single most

important factor which contributes to the stabilization of the various metal geometries and the enhancement of catalytic activities of its complexes. This ligand flexibility imposes a large degree of complex fluxionality in solution which is a subject of this paper.

A handful of semi-*closo*-bridged²¹ dppf complexes have been isolated and characterized. Single-crystal X-ray structure data for these complexes (Table 1) indicate that, despite the steric demand of the dppf ligand, it readily accommodates auxiliary bridging ligands of smaller bite size through ring and/or torsional twisting. This unusual skeletal flexibility is clearly demonstrated for the complexes listed in Table 1. For these complexes, the deviation from ideal tetrahedral geometry about the P_{*i*} (*i* = 1, 2; see Figure 1) is small for α_i , where $\alpha_i = \angle \text{C}_{\text{ipso}}(\text{Cp})\text{-P}_i\text{-M}$ containing the "ipso" in C_{ipso}(Cp). In this article, Cp is abbreviated to mean the substituted C₅H₄ rather than the conventional cyclopentadienyl C₅H₅. For $[\text{Re}_2(\mu\text{-OMe})_2(\mu\text{-dppf})(\text{CO})_6]$ ²² and $[[\text{Ag}(\text{NO}_3)(\mu\text{-dppf})]_2 \cdot 2\text{CHCl}_3]$,²³ this deviation is much larger because the significantly smaller bite angle of the auxiliary bridges reinforced the steric rigidity of the bridging fragment. The rigidity of the latter complex may also be a result of the doubly-bridging framework. Our recent isolation of the dinuclear complex $[\text{Re}_2(\mu\text{-OMe})_2(\mu\text{-dppf})(\text{CO})_6]$ demonstrates unequivocally the ability for dppf to span two metal sites without a direct M–M link but which are rigidly held by two much smaller ligand bridges such as methoxyls.²²

* Authors to whom correspondence should be addressed.

[†] On leave from the Department of Chemistry, Lanzhou University, Gansu, P. R. China.

• Abstract published in *Advance ACS Abstracts*, April 15, 1994.

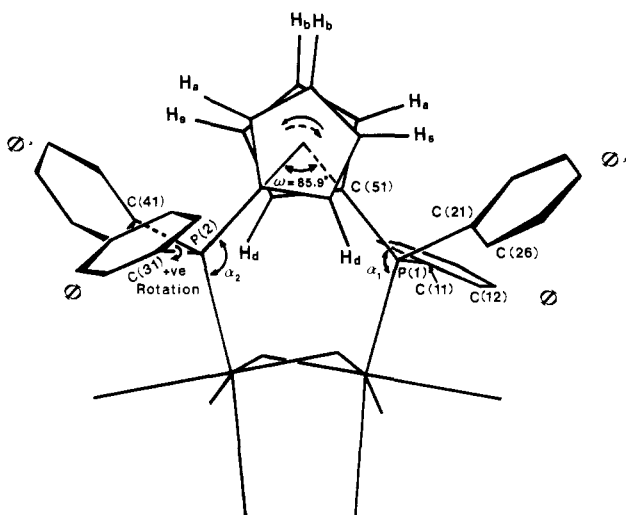
- (1) Hor, T. S. A.; Phang, L.-T. *J. Organomet. Chem.* **1989**, *373*, 319–324.
- (2) Haggerty, B. S.; Houscroft, C. E.; Rheingold, A. L.; Shaykh, B. A. M. *J. Chem. Soc., Dalton Trans.* **1991**, 2175–2184.
- (3) Baker, P. K.; Fraser, S. G.; Harding, P. *Inorg. Chim. Acta* **1986**, *116*, L5–L6.
- (4) Baker, P. K.; van Kampen, M.; ap Kendrick, D. *J. Organomet. Chem.* **1991**, *421*, 241–246.
- (5) Casellato, U.; Corain, B.; Graziani, R.; Longato, B.; Pilloni, G. *Inorg. Chem.* **1990**, *29*, 1193–1198.
- (6) Longato, B.; Pilloni, G.; Graziani, R.; Casellato, U. *J. Organomet. Chem.* **1991**, *407*, 369–376.
- (7) Kim, T.-J.; Kwon, S.-C.; Kim, Y.-H.; Heo, N. H.; Teeter, M. M.; Yamano, A. *J. Organomet. Chem.* **1991**, *426*, 71–86.
- (8) Onaka, S.; Moriya, T.; Takagi, S.; Mizuno, A.; Furuta, H. *Bull. Chem. Soc., Jpn.* **1992**, *65*, 1415–1427.
- (9) Phang, L.-T.; Au-Yeung, S. C. F.; Hor, T. S. A.; Khoo, S. B.; Zhou, Z.-Y.; Mak, T. C. W. *J. Chem. Soc., Dalton Trans.* **1993**, 165–172.
- (10) Cabri, W.; Candiani, I.; DeBernardinis, S.; Francalanci, F.; Penco, S.; Santo, R. *J. Org. Chem.* **1991**, *56*, 5796–5800.
- (11) Madin, A.; Overman, L. E. *Tetrahedron Lett.* **1992**, *33* (34), 4859–4862.
- (12) Cramer, E.; Percec, V. *J. Polym. Sci. Part A: Polym. Chem.* **1990**, *28*, 3029–3046.
- (13) Galarini, R.; Musco, A.; Pontellini, R.; Bolognesi, A.; Destri, S.; Catellani, M.; Mascherpa, M.; Zhuo, G. *J. Chem. Soc., Chem. Commun.* **1991**, 364–365.
- (14) Trost, B. M.; Scanlan, T. S. *J. Am. Chem. Soc.* **1989**, *111*, 4988–4990.
- (15) Cafagna, C.; Galarini, R.; Musco, A.; Santi, R. *J. Mol. Catal.* **1992**, *72*, 19–27.
- (16) Brown, J. M.; Cooley, N. A. *Organometallics* **1990**, *9*, 353–359.
- (17) Cabri, W.; Candiani, I.; Bedeschi, A.; Santi, R. *J. Org. Chem.* **1992**, *57*, 3558–3563.

- (18) Yoneyama, M.; Kakimoto, M.; Imai, Y. *Macromolecules* **1989**, *22*, 4152–4155.
- (19) Kalck, P.; Randrianalimanana, C.; Ridmy, M.; Thorez, A.; tom Dieck, H.; Ehlers, J. *New J. Chem.* **1988**, *12*, 679–686.
- (20) Knifton, J. F. *J. Mol. Catal.* **1988**, *47*, 99–116.
- (21) Semi-*closo*-bridged dppf complexes are defined as di- (or poly-) nuclear complexes without a direct M–M bond but where the metal centers are bridged by dppf and other co-bridging ligands.
- (22) Yan, Y. K.; Chan, H. S. O.; Hor, T. S. A.; Tan, K. L.; Liu, L. K.; Wen, Y. S. *J. Chem. Soc., Dalton Trans.* **1992**, 423–426.
- (23) Hor, A. T. S.; Neo, S. P.; Tan, C. S.; Mak, T. C. W.; Leung, K. W. P.; Wang, R. *J. Inorg. Chem.* **1992**, *31*, 4510–4516.

Table 1. Summary of Phosphorus Bond Angles α_i ($\alpha_i = \angle C_{ipso(Cp)}-P_i-M$) for Quasi-*Closo* Dppf-Bridged Complexes

complexes	α_i
[Ag ₂ (CH ₃ CO ₂) ₂ (μ -dppf)] ₂ ^a	
P(1)	113.7
P(2)	112.0
[Ag ₂ (C ₆ H ₅ CO ₂) ₂ (μ -dppf)] ^a	
P(1)	113.4
P(2)	110.8
[[Ag(NO ₃)(μ -dppf)] ₂ ·2CHCl ₃] ^a	
P(1)	116.6
P(2)	119.1
[Re ₂ (μ -OMe) ₂ (μ -dppf)(CO) ₆] ^b	
P(1)	123.4
P(2)	121.8
[Rh ₂ (μ -S- <i>t</i> -Bu) ₂ (μ -dppf)(CO) ₂] ^c	
P(1)	120.5
P(2)	109.7

^a Reference 23. ^b Reference 22. ^c Reference 19.

**Figure 1.** Labeling scheme for [Re₂(μ -OMe)₂(μ -dppf)(CO)₆].

Four interesting features are found in this complex: (a) $\alpha_1 \approx \alpha_2 \approx 122.5^\circ$, which is the largest observed for this class of complex. (b) A closely related mononuclear complex [Re(OMe)(η^2 -dppf)(CO)₃] is not formed despite the known stability of dppf as a chelating ligand and the apparent skeletal restriction of the bridging dppf on the [Re₂(μ -OMe)₂] core. Recent isolation of the analogous complex [Re(OMe)(η^2 -dppe)(CO)₃]²⁴ proves the stability of this mononuclear configuration. (c) Fluxionality of the complex is reflected in, and confined to, the phenyl and Cp protons with the [Re₂(μ -OMe)₂] core remaining essentially static. (d) The Cp proton NMR resonances spread over an unusually large region between 3.0 and 5.7 ppm. All these peculiarities are related to the stereoproperties of dppf as a bridging ligand. This complex thus provides a suitable model for a detailed investigation of the solution dynamics of dppf in its semi-*closo* bridging state. The A-frame chemistry of alkyl-chained diphosphines especially dpmm is rich and diverse.²⁵ Similar dimetal chemistry of dppf is insofar undeveloped; its future prospect depends largely on the dynamic properties in relation to the metal cooperative effect of the ligand. A sample of the literature work revealed a host of fluxionality studies of chelating dppf.³⁻⁸ In-depth conformational analysis of bridging dppf is rare though recently the rocking motion of the dppf ligand between two metal centers has been recognized.²⁶⁻²⁸

(24) Mandal, S. K.; Ho, D. M.; Orchin, M. *Inorg. Chem.* **1991**, *30*, 2244-2248.

(25) Chaudret, B.; Delavaux, B.; Poiblan, R. *Coord. Chem. Rev.* **1988**, *86*, 191-131.

(26) Housecroft, C. E.; Rheingold, A. L. *Organometallics* **1987**, *6*, 1332-1340.

Experimental Section

All ¹H and ¹³C NMR spectra were recorded on a Bruker WM-250 superconducting FT-NMR spectrometer operating at 250.13 and 62.86 MHz, respectively. The chemical shift was reported in ppm units from internal TMS. For the variable-temperature ¹H NMR experiments, spectra were collected after the sample was equilibrated for 1 h. The COSY and EXSY experiments were carried out using the standard COSY-90 and NOESY sequence. The mixing time for the EXSY experiment was 0.4 s. For data treatment, a sine bell window function was used with a 0° shift for both dimensions. Appropriate zero-filling was carried out in the second dimension prior to Fourier transformation. ¹³C spectral editing was carried out using standard DEPT sequence.

All molecular modeling calculations were conducted using the CHEM-X program (PC release) licensed from the Chemical Design Ltd., Oxford, England. Davies *et al.*²⁹⁻³² have successfully demonstrated that accessible conformational space can be generated through an analysis based on the assumption of correlated rigid rotor rotations. This type of analysis has proven to provide a reasonable explanation for observed conformations in solution. [Re₂(μ -OMe)₂(μ -dppf)CO₆] was constructed using single-crystal X-ray structure data.²² Dummy atoms were used for Re and Fe because of the lack of adequate metal parametrization. Since steric influences from Fe atom were assumed to be negligible,²⁹⁻³² contributions from steric effects to the potentials from Fe and Re atoms were neglected in the calculation. The van der Waals (vdW) interaction energy of the system sums the contribution arising from the electrostatic (E_{ele}), polarization (E_{pol}), and torsional (E_{tor}) energy terms.³³ Their explicit forms are given as follows:

$$V_{el} = \frac{KQ_1Q_2}{\epsilon r} \quad (1)$$

$$V_{nb(pol)} = \frac{Ae^{-Br}}{r^D} - \frac{C}{r^6} \quad (2)$$

$$V_{tor} = T_{nc}(1.0 + \cos 3\omega) \quad \text{nonconjugated bonds} \quad (3)$$

$$V_{tor} = T_c(1.0 - \cos 2\omega) \quad \text{conjugated bonds}$$

$$V_{tor} = T_d(1.0 - \cos 2\omega) \quad \text{double bonds}$$

In eq 1, K is a unit conversion factor, Q_1 and Q_2 are the partial charges, ϵ is the dielectric constant (or dielectric function), and r is the interatomic distance. In eq 2, A - D are constants, whereas r is the internuclear distance in Å. In eq 3, T_{nc} is the nonconjugated barrier for the central atom pair, T_c is the conjugated barrier for the central atom pair, and T_d is the double-bond barrier for the central atom pair, while ω is the torsion angle.

Results and Discussion

Assignments for the ¹H and the ¹³C NMR spectra of [Re₂(μ -OMe)₂(μ -dppf)(CO)₆] are summarized in Table 2. The downfield ¹³C shift for the methoxy group ($\delta(^{13}\text{C}) = 73.65$ ppm) compared to that found in [Re(OMe)(dppe)(CO)₃] ($\delta(^{13}\text{C}) = 67.2$ ppm²²) indicates a reduction in the nucleophilicity of the oxygen upon conversion from terminal methoxy to its bridging state. For the Cp protons at $\delta(^1\text{H}) = 3.64$ and 4.78 ppm, additional broadening was observed going from 60 to 250 MHz. Therefore,

(27) Harpp, K. S.; Housecroft, C. E. *J. Organomet. Chem.* **1988**, *340*, 389-396.

(28) Draper, S. M.; Housecroft, C. E.; Rheingold, A. L. *J. Organomet. Chem.* **1992**, *435*, 9-20.

(29) Davies, S. G.; Blackburn, B. K.; Whittaker, M. *Stereochemistry of Organometallic and Inorganic Compounds*; Bernal, I., Ed.; Elsevier: Amsterdam, 1989; Vol. 3, pp 141-223.

(30) Davies, S. G.; Seeman, J. I.; Williams, I. H. *Tetrahedron Lett.* **1986**, *27*, 619-662.

(31) Davies, S. G.; Blackburn, B. K.; Sutton, H.; Whittaker, M. *Chem. Soc. Rev.* **1988**, *17*, 147-179.

(32) Davies, S. G.; Derome, A. E.; McNally, J. P. *J. Am. Chem. Soc.* **1991**, *113*, 2854-2861.

(33) (a) *CHEM-X Reference Guide*; Chemical Design Ltd.: London, 1993; Vol. 2, Chapter 14. (b) *CHEM-X User Guide*; Chemical Design Ltd.: London, 1992; Chapters 10 and 11.

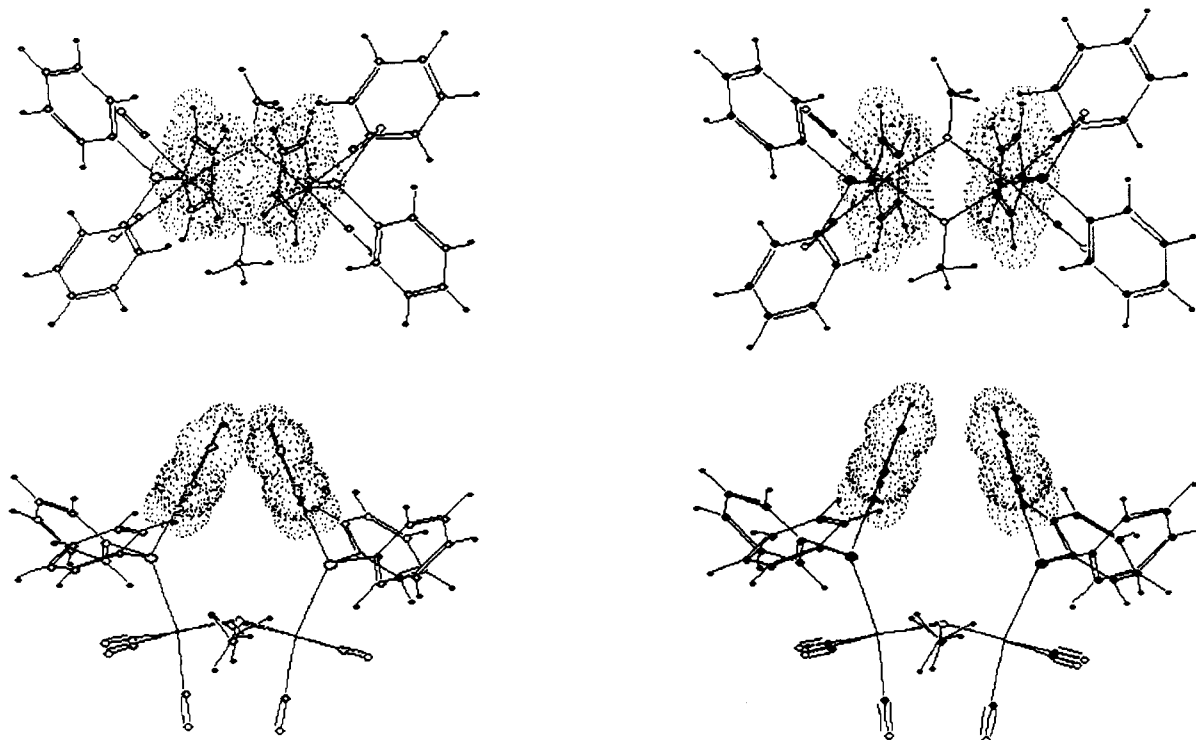


Figure 2. Suggested side and top view (a, left) $\alpha_{1,2} = 136^\circ$ and (b, right) $\alpha_{1,2} = 142^\circ$ of the structure of $[\text{Re}_2(\mu\text{-OMe})_2(\mu\text{-dppf})(\text{CO})_6]$ passing from *R* to the *S* forms.

Table 2. Summary of NMR Data in CD_2Cl_2 Solution

$\delta(^1\text{H})/\text{ppm}$		$\delta(^{13}\text{C})/\text{ppm}$	assgnt
298 K	228 K		
7.45 (bs) ^a	7.05–7.38	73.65 ^c	phenyl protons $\mu\text{-CH}_3\text{O}$ group Cp protons
4.60 (s) ^b	4.60		
3.64 (b) ^d	3.00 (H_s)		
	4.20 (H_b)		
4.78 (b) ^d	3.89 (H_a)		Cp protons
	5.68 (H_d)		

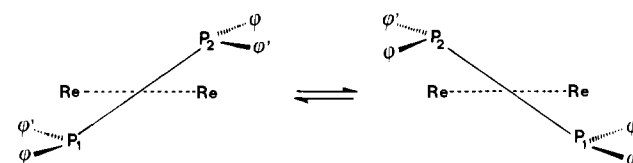
^a bs = broad singlet. ^b s = singlet. ^c This assignment is supported by DEPT experiments at 228 K. ^d b = broad.

the fluxionality of Cp was examined since conformational exchange has been well established for metal complexes containing the dppf ligand system.²⁴ The variable-temperature experimental results confirmed the fluxional properties of dppf. At 228 K in CD_2Cl_2 , the exchanging Cp protons were frozen out giving four well-resolved peaks labeled H_s , H_a , H_b , and H_d at $\delta(^1\text{H}) = 3.00$, 3.89, 4.20, and 5.68 ppm, respectively. The phenyl absorptions were split into two sets of asymmetrical broad doublets. No changes in the methoxy peak was detected throughout the temperature-lowering process. This particular result indicates the following: (i) The structural integrity (rigidity) of the methoxy-bridged core ($[\mu\text{-OMe-Re}]_2$) was retained in solution and was unaffected by the fluxional process. In the solid, the structural data demonstrated that the two methoxy ligands are symmetrically disposed between the two Re(I) centers with the average distance of $\text{Re-O} = 2.163(6)$ Å and $\text{Re-O-Re} = 103.83(23)^\circ$. (ii) Little or no geometrical or electronic changes take place at the Re(I) centers as a result of the fluxional process. (iii) The fluxionality shown by the ferrocenyl fragment was unusually high. An average activation energy of 46.4 ± 1.0 kJ/mol was calculated from the four peaks (Table 3) for the barrier to exchange. Fluxionality of the ferrocene similar to those in CD_2Cl_2 was also observed in CDCl_3 and d_6 -benzene. It was also observed that the phenyl rings remained dynamical in all three solvents at 195 K. During the freeze out process, peak cross-over occurred. Combined 2-D EXSY and ^1H - ^1H COSY experiments conducted at 228 K established that H_s , H_a , H_b , and H_d all belong

Table 3. Summary of ΔG^\ddagger Values in CD_2Cl_2 for Cp Protons

Cp proton	$\Delta G^\ddagger/\text{kJ mol}^{-1}$
H_s (3.00 ppm)	45.7
H_a (3.89 ppm)	47.9
H_b (4.20 ppm)	45.9
H_d (5.68 ppm)	46.1
	46.4 ± 1.0 (mean)

Scheme 1



to the same Cp and the two exchanging proton pairs are H_a , H_d and H_b , H_s . The assignment for the Cp protons is summarized in Table 2. The designation for the Cp protons and phenyl rings ϕ and ϕ' is given in Figure 1. The expected J coupling is small ($^1J \approx 1.5$ Hz) compared to the line width of the protons ≈ 6 Hz; therefore, couplings were not resolved.

Figure 1 was constructed using the CHEM-X program based on the published²² single-crystal X-ray structure data of $[\text{Re}_2(\mu\text{-OMe})_2(\mu\text{-dppf})(\text{CO})_6]$. Two prominent features are noted: (i) ϕ and ϕ' were oriented 21.5° with respect to each other and (ii) the Cp-Fe-Cp axis of dppf fragment is twisted by 53.5° with respect to the Re...Re axis. If the "frozen" structure corresponds closely to that of the single-crystal X-ray structure, the ferrocene fragment of the dppf ligand in the complex adopts the synclinal³⁴ (gauche) conformation. The relative orientation of the two Cp rings is $\omega \approx 85.9^\circ$ ($+13.9^\circ$ from an ideal gauche eclipsed conformation; see Figure 1). Therefore, the molecule has no symmetry plane. The conformers of $[\text{Re}_2(\mu\text{-OMe})_2(\mu\text{-dppf})(\text{CO})_6]$ are enantiomeric with magnetically distinct phenyl groups. The pathway for the interchange of the *R* and *S* forms (Scheme

(34) For a five-membered ring system, there are two idealized "synclinal (or gauche)" conformations, *viz.* staggered ($\omega 36^\circ$) and eclipsed ($\omega 72^\circ$).

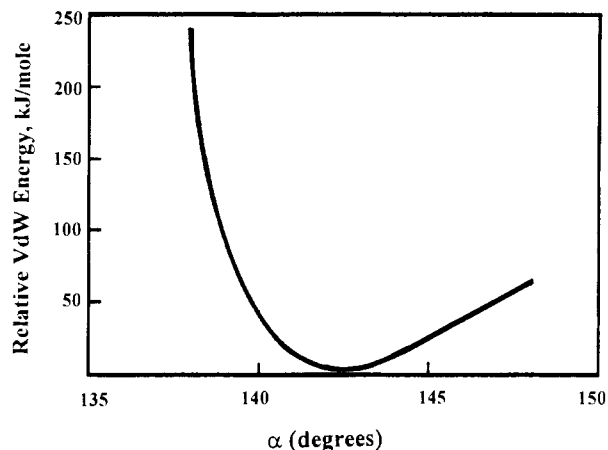


Figure 3. Plot of the relative vdW Energy versus α (deg) showing the angular dependence of the vdW Energy with $\angle C_{Cp(ipso)}-P-M$.

1) can be visualized through the opposite twisting of the two halves of the ferrocene sandwich about the Cp-Fe-Cp centroid axis coupled with the correlated torsional twist about the P-C_{ipso}(Cp) and the P-Re bonds. The low-temperature ¹H NMR spectrum confirmed the static [ABCD]₂ pattern for the Cp protons. Similar rocking motion has been recently advocated by Housecroft *et al.* on a [Au₂M₄B] (M = Fe,^{26,27} Ru²⁸) cluster core.

For the conversion of the *R* to the *S* form, ϕ and ϕ' must be identical during barrier crossing. This requirement is met when the Cp centroid-centroid axis (r_{c-c}) is coplanar with the virtual P-P or the Re-Re axis. Although this structure can be obtained by rotation of both the P-Re and C_{Cp(ipso)}-P bonds, overlapping of the Cp electron cloud results within the approximation of the CPK³⁵ model. Without increases in α_i , r_{c-c} is greatly reduced below 3.28 Å (centroid to centroid separation of the two cyclopentadienyl rings obtained from X-ray data) and the model is not meaningful. Marginal separation of the CPK clouds is obtained at $\alpha_{1,2} = 136^\circ$ (Figure 2a). The corresponding $r_{c-c} \approx 2.75$ Å determined by measurement of the centroid to centroid distance remains significantly shorter than 3.28 Å and the relative vdW is unrealistically high. Further increase of $\alpha_{1,2}$ to $\approx 142^\circ$ is necessary to avoid overlapping of the Cp ring cloud, while r_{c-c} is maintained at the optimized separation of 3.28 Å (Figure 2b). The minimum on the plot of the relative vdW energy versus α (Figure 3) correspond to this structure. At $\alpha_{1,2} = 142^\circ$, the corresponding r_{c-c} (≈ 3.34 Å) is in good agreement with the ideal r_{c-c} of 3.28 Å. Therefore, both constraints were met simultaneously. The combined effects of tilting the Cp planes together with variation in α resulted in no significant improvements in the relative vdW energy, in the separation of the CPK cloud, or in the optimization of r_{c-c} toward 3.28 Å. The large increase ($\approx 20^\circ$ from 122°) in $\alpha_{1,2} \approx 142^\circ$ necessary to reach a vdW energy minimized structure during barrier crossing is questionable although some support can be derived from the values of the α_i ($>109.5^\circ$) for similar semi-*closo*-bridged complexes collected in Table 1. We suggest that the transformation of the *R* to *S* forms is unlikely by passage over the barrier. Probably, quantum mechanical tunneling through the barrier is more plausible.

To account for the large Cp proton shifts at 228 K, the dynamics of ϕ and ϕ' in [Re₂(μ -OMe)₂(μ -dppf)(CO)₆] were studied by following the well-established conformational analysis method set out by Davis²⁹⁻³¹ using CHEM-X. The conformational calculations were restricted to intramolecular dynamic processes involving only ϕ and ϕ' . All other groups bound to the phosphorus remain fixed because the rotation motions of the methoxy groups and the carbonyl groups are sufficiently far away from ϕ or ϕ' to affect their dynamic properties. Therefore, they can be

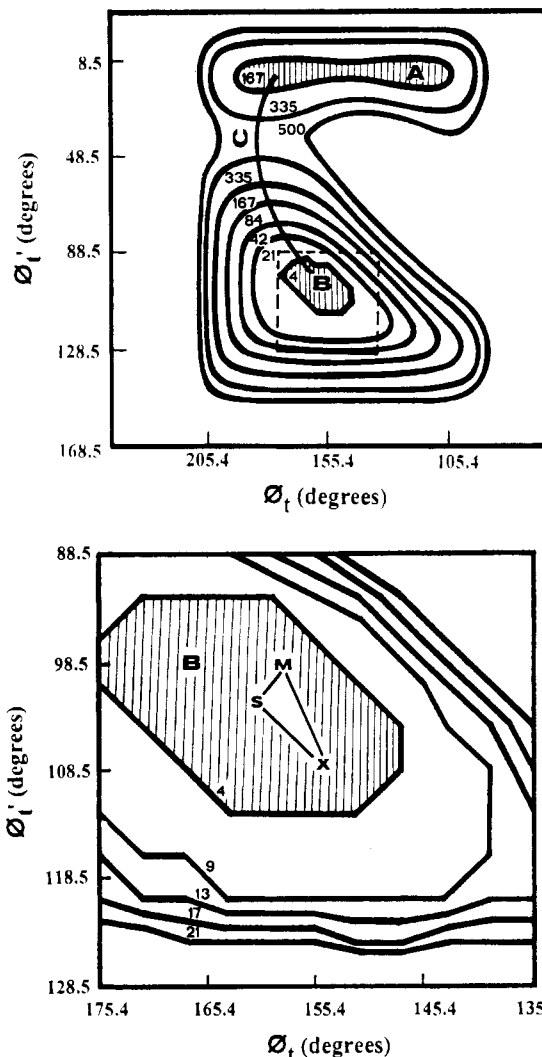


Figure 4. Conformational energy contour (kJ) diagram for ϕ_t' ($\angle C(26)-C(21)-P(1)-C(51)$) and ϕ_t ($\angle C(12)-C(11)-P(1)-C(51)$) generated using CHEM-X. (a) Top: Full 180° range for both ϕ_t' and ϕ_t . (b) Bottom: Expansion of conformation contours corresponding to the square (broken line) defined in (a).

neglected from the conformational analysis. Four C_{ipso}(phenyl)-P bonds, namely, C(21)-P(1), C(41)-P(2), C(11)-P(1), and C(31)-P(2), were considered in the calculation. The conformational energy surface created by ϕ and ϕ' was generated by arbitrarily setting, e.g. ϕ , in a fixed orientation and driving ϕ' through 360° . By repetition of this procedure for other angles of ϕ in 5° increments, the resulting nonbonded conformation energy contours are shown in Figure 4a. The region defined by the square box (broken line) in Figure 4a is expanded in Figure 4b. All calculated nonbonded energies were rounded off to the first decimal place with the lowest value arbitrarily set to zero on the energy scale. In Figures 4a,b, counterclockwise rotation about the C_{ipso}(phenyl)-P bond for both ϕ and ϕ' corresponds to increasing torsional angles defined by $\phi_t = C(12)-C(11)-P(1)-C(51)$ and $\phi_t' = C(26)-C(21)-P(1)-C(51)$, respectively, and is illustrated in Figure 1. The two conformation wells are shown in gridded areas labeled "A" and "B" in Figure 4a. The high-energy valley located below ≈ 167 kJ/mol (gridded area "A") corresponds to the conformation in which the phenyl protons are sandwiched between the Cp rings (Figure 5). The lowest energy pathway connecting "A" and "B" was determined to follow line "C" in Figure 4a. The highest point (barrier) along "C" was determined to be ≈ 400 kJ/mol. The remaining discussion focuses on "B" whereby all conformation states defined by the contour below 4 kJ/mol were fully accessible.

(35) The CPK radius—hard sphere space-filling of individual atoms—was chosen for the study of the cloud effects.

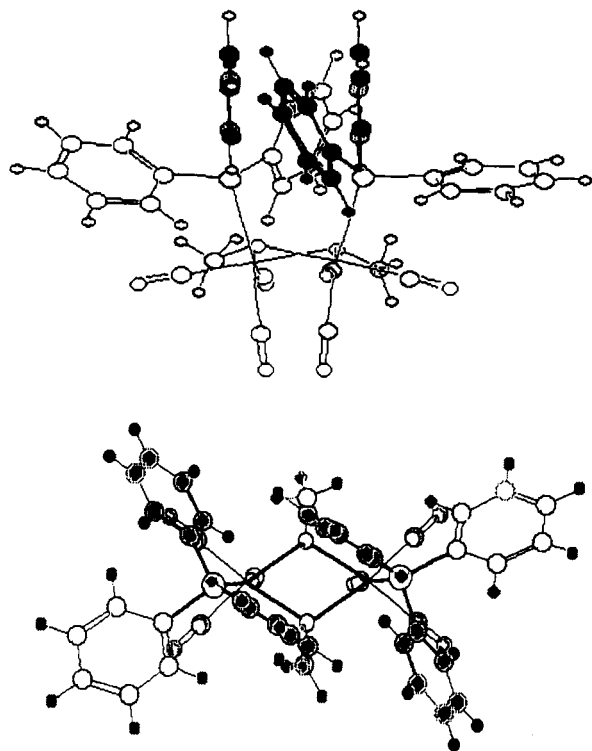


Figure 5. Orientation of ϕ or ϕ' corresponding to grided area A in Figure 4a: (a, top) top view; (b, bottom) side view.

For the energy minimization procedure, the optimum orientations of ϕ_t and ϕ'_t were determined by initially setting the plane of the phenyl rings vertically relative to the Cp planes.²⁹ The torsional angles ϕ_t and ϕ'_t equal 158.6 and 99.3°, respectively, in the energy-minimized structure. This structure marked by "M" in Figure 4b corresponds to the conformation generated by ϕ and ϕ' as ideal rotors. In Figure 4b, the contour at 4 kJ/mol defines the boundary for the rotation motion of the C_{ipso}-P bond for ϕ and ϕ' . The rotational limits, 92.6° ≤ ϕ'_t ≤ 112.4°, was determined for ϕ' . Similarly, ϕ was determined to oscillate between the limits 147.6° ≤ ϕ_t ≤ 177.8°. Rotation of ϕ and ϕ' is determined to be opposite for strain relief because of ring cloud repulsion. On the basis of the rotation limits of C_{ipso}(ϕ, ϕ')-P in mobile solution at 228 K, the average torsional angles were obtained, i.e. $\phi_t \approx 162.7^\circ$ and $\phi'_t \approx 102.5^\circ$. The average conformation determined by this procedure is located at the center of the potential well marked by the point "S" in Figure 4b. In the crystal form, $\phi_t = 155.4^\circ$ was determined for ϕ and $\phi'_t = 108.5^\circ$ for ϕ' . This point is marked by "X" in Figure 4b. This conformation was ≈ 1 kJ/mol higher than the lowest energy conformation generated. The difference in the torsional angles determined between solid and solution was small and is attributed to packing effects. Therefore, the X-ray structure is confirmed to be thermodynamically the lowest energy conformation. Given the large number of approximations inherent in the use of modeling techniques, the agreement between the values of the torsional angles using the procedures described above compared to the values determined by single-crystal X-ray is excellent. The triangle in Figure 4b defined by the three points "X", "S", and "M" bracketed the true values for ϕ_t and ϕ'_t in solution.

The distances of the respective Cp protons from ϕ or ϕ' were readily obtained from the torsional rotation limits for the C_{ipso}(ϕ, ϕ')-P bonds. From the spatial orientation of the Cp protons at the torsional limits for ϕ' (Figure 6), it was determined that neither H_a nor H_b was in the proximity of either ϕ or ϕ' . Consequently, normal Cp proton chemical shifts were expected and were confirmed experimentally. The average distance of H_s was determined to be ≈ 2.86 Å above the π -cloud of ϕ' . Aside from ring current effects which led to shift of H_s to high field,

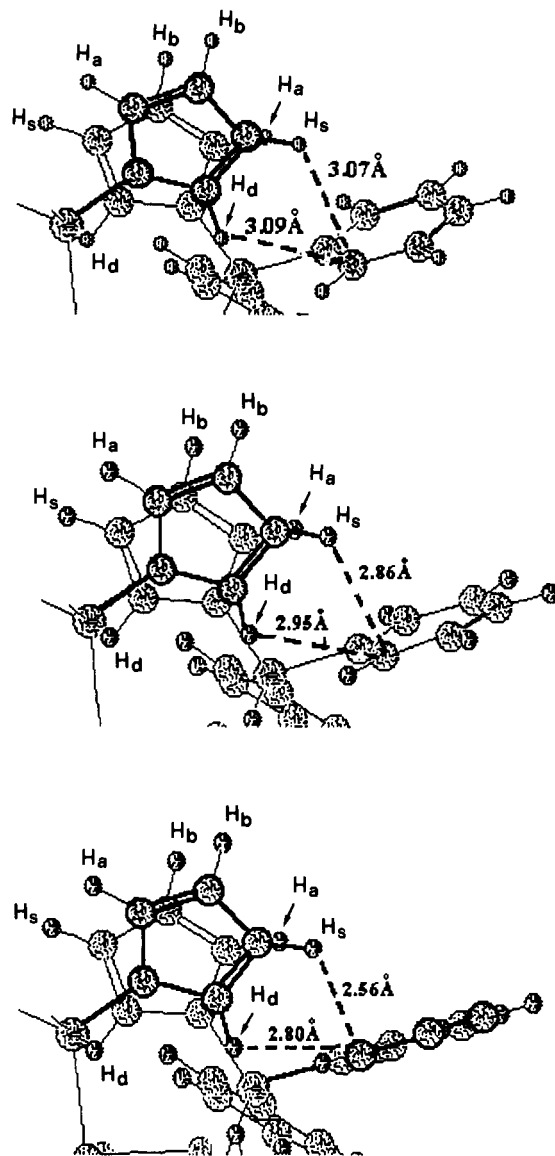


Figure 6. Structural representations showing the spatial orientation of the Cp protons and the intramolecular interligand H_{s,d}(Cp)- ϕ' (plane) distances with respect to the three rotational limits for the C_{ipso}-P bonds.

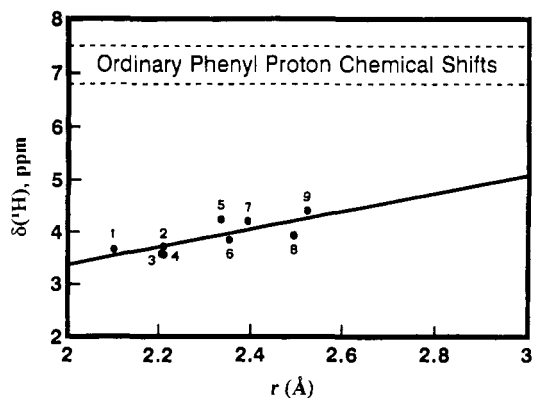
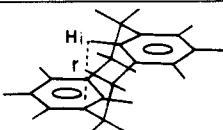
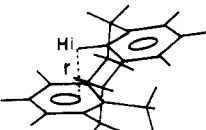
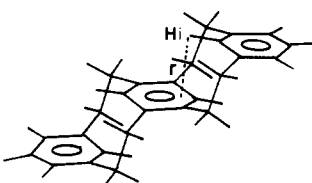
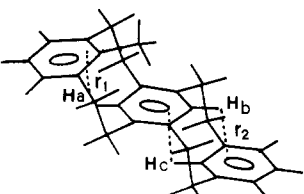
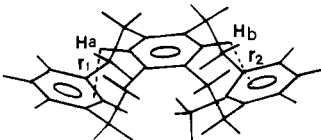
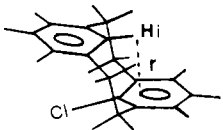


Figure 7. Plot of $\delta(^1\text{H}_s)$ versus r for cyclophanes. Data were tabulated in Table 4. Key: (1) Compound E, H_a; (2) compound B; (3) compound D, H_b; (4) compound E, H_b; (5) compound A; (6) compound D, H_a; (7) compound D, H_c; (8) compound F; (9) compound C.

there is no spectroscopic evidence suggesting H_s interacts with the π electron cloud of the phenyl ring in the form of CH/ π interaction.^{36,37} The magnitude in the upfield shift for H_s is similar

(36) Nishio, M.; Hirota, M. *Tetrahedron* 1989, 45, 7201-7245.

Table 4. Summary of ^1H NMR Data for Cyclophanes^a

compd	structure	$\delta(\text{H}_i)/\text{ppm}$	$r/\text{\AA}$
A		4.25	2.34
B		3.72	2.21
C		4.41	2.52
D		3.85 (H _a) 3.59 (H _b) 4.21 (H _c)	2.35 2.20 2.39
E		3.67 (H _a) 3.57 (H _b)	2.10 2.21
F		3.94	2.49

^a Reference 38.

to the upfield shift phenomenon observed for the internal proton, H_i , in cyclophane molecules. Ring current effects has been established to be the origin responsible for the shifts of H_i when situated above the π -cloud. The H_i proton chemical shifts depends on its distance r (the perpendicular distance between the proton and the ring plane) above the π -cloud; the shorter the distance, the more pronounced the upfield shift. Figure 7 gives the plot of $\delta(^1\text{H}_i)$ versus r for the cyclophanes collected in Table 4. The

cyclophanes were constructed using data³⁸ from solid-state and/or standard bond lengths and angles using CHEM-X. The distance r was measured when the energy minimized structure was obtained. For ordinary phenyl protons, $\delta(^1\text{H}) \approx 6.8\text{--}7.5$ ppm (Figure 7). When $r \approx 3$ Å, as much as 1.5 ppm shift to upfield could be expected for normal phenyl protons. Therefore, the observed upfield shift of 1 ppm from ≈ 4 ppm (normal Cp proton chemical shifts) for H_s ($\delta(^1\text{H}) = 3.00$ ppm) is readily rationalized on the basis of the analysis built upon the internal proton (H_i) chemical shifts observed for cyclophanes.

The rotation restriction of ϕ' at 228 K ensures that H_d , always sitting in the quasi-*closo*-dibridged cavity, maintains a position within very close proximity to the deshielding region of ϕ' . The average distance of H_d from the nearest carbon atom on ϕ' was determined to be 2.95 Å. Again, ring current effects accounts for the large proton shift to low field. Downfield shift of one of the α -protons, H_d , has also been observed in the $[\text{HRu}_4(\text{CO})_{12}\text{-BAu}_2(\text{dppf})]$ cluster ($\delta(^1\text{H}) = 5.37$ ppm²⁸) when it is pointing toward the $[\text{Au}_2\text{P}_2]$ cavity. It is anticipated that ring current effects are also operative. The observed shift in the present complex ($\delta(^1\text{H}) = 5.68$ ppm) is to our knowledge the largest shift for reported Cp resonances.

Conclusion

Previous works have already identified the rotational motions of the Cp rings, inversion and vertical movements of the phosphorus atoms, and twisting motion of the ferrocenyl skeleton with respect to the dimetal entities.⁷⁻¹⁰ The present work enables an illustration of these fluxionalities through an NMR conformational analysis. It also for the first time reveals the spectroscopic and geometrical impact of the phenyl rotations. These rotations, in conjunction with the ferrocenyl mobilities, allow the dppf ligand to seek and adopt a most suitable conformation between two metal centers. That such a comfortable stereoposition can be found irrespective of the metal environment and other complex core behavior is a vital prerequisite for this ligand to function effectively in a changeable role. The stability of the dppf ligand on the rigid $[\text{Re}_2(\mu\text{-OMe})_2]$ core with respect to dissociation to give the mononuclear chelate form is a consequence of this ligand adaptability. An important lead of this work lies in the analysis of other diphosphine complexes whose catalytic activities are believed to be conformationally related. The advantage of the dppf ligand as an active probe for NMR analysis of phosphine complexes can be envisaged.

Supplementary Material Available: Figures showing ^1H NMR, 2D EXSY, and 2D COSY-90 spectra (3 pages). Ordering information is given on any current masthead page.

(37) Sakakibara, K.; Hirota, M. *Chem Lett*. 1989, 921-924.(38) Keehn, P. H.; Rosenfeld, S. M., Eds. *Cyclophanes*; Academic Press: New York, 1983; Vols. I and II.